COASTAL FLOODING RISK ASSESSMENT USING SPATIAL MULTI-CRITERIA DECISION ANALYSIS IN THE SELECTED CITIES OF BANGLADESH

Aysha Akter[1*], S. M. Ataullah[2]

[1] Department of Civil Engineering, Chittagong University of Engineering & Technology (CUET), Chittagong 4349, Bangladesh, e-mail: aysha_akter@cuet.ac.bd
[2]Department of Water Resources Engineering, Chittagong University of Engineering & Technology (CUET), Chittagong 4349, Bangladesh, e-mail: sm_ataullah@yahoo.com

***Corresponding Author**

ABSTRACT

Coastal regions face an elevated threat of inundation due to the combination of rising sea levels attributed to climate change and intermittent surges in sea levels. Within this coastal zone, two prominent sandy beaches highly valued by tourists, namely Patenga and Cox's Bazar, are situated. Previous studies have concentrated on assessing flood hazards to aid decision-makers in implementing suitable mitigation strategies. Nevertheless, a holistic flood risk management approach should account for other components of risk, namely vulnerability and exposure, aspects often overlooked in these studies. Flood Susceptibility Mapping (FSM) has been widely utilized. Nevertheless, these methods overlook the crucial aspects of hazard, vulnerability and exposure assessment within coastal flood risk. Quantitative techniques, i.e., probabilistic methods, are commonly employed for flood risk assessment. This study has introduced a semi-quantitative approach founded on spatial multi-criteria decision analysis (SMCDA) to bridge this gap and integrate with factors responsible for triggering coastal flooding incidents in Chattogram and Coxs' Bazar, Bangladesh. Then, hazard, vulnerability, and exposure were included in a hierarchical framework with indicators and proxy variables. An AHP model is also implemented to assign weights for the various indicators associated with hazard, vulnerability and exposure components. This study delineates flooded areas in five distinct categories. Among the five vulnerability classes, very low, low, moderate, high and very high zones cover about 25.67%, 16.16%, 27.97%, 19.79% and 10.41%, respectively. These findings can guide decision-makers in implementing appropriate strategies for reducing risk in high-risk coastal flood zones. Under this assessment, 8.23% of the study area was found to be a high-risk flooding zone. The reported study was evaluated with the Area Under the Curve (AUC) and acquired a reasonable outcome for the decision support system.

Keywords: *Coastal-flood; GIS; Risk; SMCDA; AHP.*

1. INTRODUCTION

Floods stand out as one of the most destructive natural calamities compared to other disasters. They wreak havoc on communication infrastructure and properties, leading to substantial human and livestock casualties and the devastation of agricultural produce, farmlands, and crucial assets (Ahmed et al., 2018). Coastal flooding is a widespread global phenomenon, influenced by climatic conditions, geographical factors, the environment, human activities, and other elements (Wheater, 2006). Natural and formidable, coastal flooding poses a significant ongoing challenge for human societies due to its potent and widespread destructive impact (Teng et al., 2017). Thus, flood threats are projected to persist, and as climate change continues, the frequency and intensity of floods are expected to become a problem in many parts of the world. Bangladesh, characterized by low-lying terrain, has grappled with recurring flooding disasters over time (Hossain & Adhikary, 2022). Floods in Bangladesh result from various factors, including excessive rainfall, the country's low topography, and flat slopes. The geographic location, influenced by the southwest monsoon from the Himalayas, coupled with the convergence of major rivers (Ganges, Brahmaputra, Meghna), contributes to heightened flood risks and the presence of 405 major and minor rivers, along with artificial alterations like embankments and unplanned infrastructure, exacerbates flooding (Adnan et al., 2019). Tidal influences, cyclones, and long-term environmental changes, such as climate variations and deforestation, further influence the occurrence and intensity of floods in the region (Abbass et al., 2022; Murshed et al., 2022). The coastline spans 710 km, parallel to the Bay of Bengal (CZPo, 2005). As per the Government of Bangladesh's Coastal Zone Policy (CZPo, 2005), 19 out of 64 districts fall within the coastal zone, with only 12 directly meeting the sea or lower estuary. According to UNICEF's report, this year, floods in Chattogram have affected 843,505 people (401,959 women and 292,214 children). 28,070 homes are concerned, of which 18,885 are partially damaged and 9,185 are completely damaged (UNICEF, 2023). About 85,500 people—including 3,500 children and 3,974 Rohingya refugees—were displaced as a result of the floods that affected nearly 538,373 people in Cox's Bazar (including 25,533 in Rohingya camps and 185,200 children), who sought safety in makeshift flood shelters (UNICEF, 2023). Several studies utilize diverse and comprehensive methods for Flood Susceptibility Mapping (FSM), e.g. multi-criteria decision analysis (Souissi et al., 2020), logistic regression (Pradhan, 2009), frequency ratio approach (Siahkamari et al., 2018), the weight of evidence equations (Tehrany et al., 2017), k-nearest neighbor logic (Liu et al., 2016), analytic network process framework (Dano et al., 2019), and Bayesian network fusion technique (Li et al., 2019). The prior studies have focused on evaluating flood hazards in order to assist decision-makers in putting appropriate mitigation techniques into place. However, other risk factors, such as exposure and susceptibility, are often overlooked in those studies. This study presents a semi-quantitative approach, spatial multi-criteria decision analysis (SMCDA), primarily grounded in the AHP model. Utilizing a GIS-based SMCDA approach allows for resolving intricate decisions through hierarchical structuring, determining the relative significance of criteria, and systematic incorporation (Malczewski, 2006). To evaluate flood risk, a GIS-based SMCDA method using the AHP model is created for the two major coastal cities of the eastern coastal zone of Bangladesh: Chattogram and Cox's Bazar. This method integrates three crucial risk components—flood hazard, vulnerability, and exposure to produce comprehensive risk maps. Unlike prior studies, this research offers two critical policy implications for legislators and urban planners; the first one is for the assessment of vulnerability utilizing indicators along with hazard and exposure components to determine the risk of flooding; the second is to offer a quick flood risk assessment method that gives coastal planners and decision-makers information for better planning in the future.

2. STUDY AREA PROFILE

Two administrative districts, Chattogram and Cox's Bazar, are selected for the current study (Figure 1). These two districts are located in the eastern coastal region of Bangladesh (i.e., 22.3569° N, 91.7832° E and 21.4272° N, 92.0058° E, respectively). According to the most recent Population and Housing Census (BBS, 2023), the total area of these two districts is around 7665 sq km. From spatial land use land cover (LULC) classification data for the study, it is found that about 31% is agricultural land, and 34% is the buildup area of these two districts. The extensive sandy beach, stretching 145 km from Cox's Bazar to Teknaf, results from the region's submerged sand. (Bhuiyan et al., 2020).

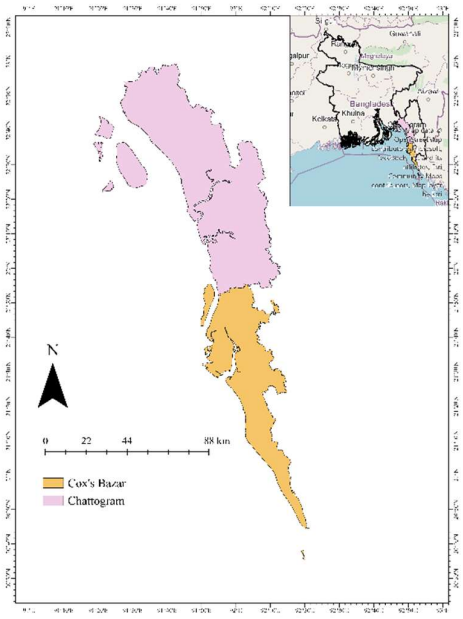

Figure 01: The Study Area Map

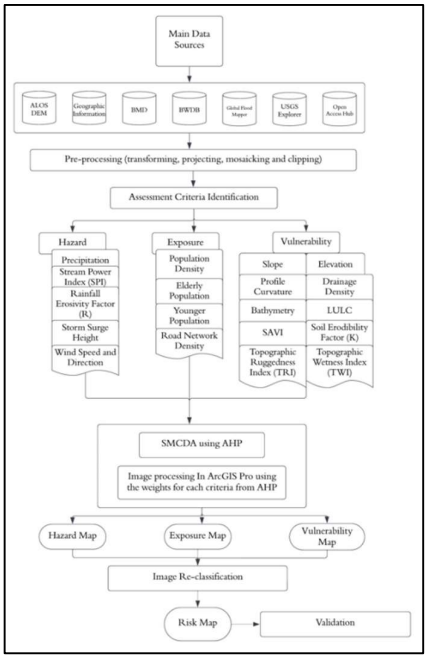

Figure 02: Methodology flow chart of the study

3. METHODOLOGY

The required three critical components in this study are: (i) hazard, incorporating factors contributing to coastal flooding (ii) vulnerability, reflecting the degree to which people are vulnerable to or unable to handle, react to, or recover from hazard events reflecting the degree to which people are vulnerable to, or unable to handle, react to, or recover from hazard events (Field et al., 2012) and (iii) exposure: pertains to the list of elements within a specific area where hazard events might take place (Basher, 2009) (Figure 2). To compute the coastal flooding risk index, this study has used the Hadipour et al. (Hadipour et al., 2020) equation, i.e.,

$$\text{Flood risk} = \text{Hazard} \times \text{Vulnerability} \times \text{Exposure} \quad (1)$$

Then, evaluating the risk of coastal flooding was conceptualised using a SMCDA framework, facilitating risk analysis through the integration of extensive temporal and spatial data (Malczewski, 2006). Next, weights were assigned to risk indicators, and proxy variables were normalised using the AHP and min-max techniques. To map flood risk, weighted indicators and normalised proxy variables were integrated using various geographic methods.

3.1 Indicators Selection and Interpolation

3.1.1 Hazard Indicators

As per the expert consensus, indicators related to hazards encompassing storm surge inundation, stream power index (SPI), rainfall erosivity factor (R), and wind speed setup were recognized for flood hazard mapping. Here, a 12.5 m spatial resolution ALOS PALSAR Digital Elevation Model (DEM) from the Alaska Satellite Facility Distributed Active Archive Data Center (ASF DAAC) was utilized to simulate storm surge inundation. The SPI reflects the intensity of erosive processes induced by surface runoff

(Jaafari et al., 2014; Rahmati et al., 2019). The required calculation involves the catchment area and slope of a specified region, as expressed in Equation (2) (Rahmati et al., 2019):

$$SPI = [\ln(A_s + 0.001) \times ((\frac{\beta}{100}) + 0.001)] \quad (2)$$

Where, A_s is the basin flow accumulation, β is the basin slope.

Slope was produced in ArcGIS Pro 3.2 using the ALOS DEM. Data on wind speed and precipitation, both daily and monthly, were gathered from the Bangladesh Water Development Board (BWDB) and Bangladesh Meteorological Department (BMD) between 2012 and 2022. The rainfall erosivity factor (R) was calculated following Morgan (Morgan, 1974) Equation:

$$R = 9.28P - 8838.15 \times I_{30} \quad (3)$$

Where, P is the average rainfall and I_{30} is 75 mm/hh^{-1}

3.1.2 Vulnerability Indicators

Following available literatures, expert opinions, and considering data accessibility, ten indicators were selected e.g. slope, elevation, profile curvature, drainage density, topographic ruggedness index (TRI), bathymetry, LULC, topographic wetness index (TWI), soil erodibility factor (K), soil-adjusted vegetation index (SAVI) (Ali et al., 2023; Cai et al., 2021; Danumah et al., 2016; Hadipour et al., 2020) are used in this study. Slope, elevation and profile curvature are prepared in GIS environment (ArcGIS Pro 3.2) from the DEM data. The drainage density (D_d) was also extracted from DEM and stream network data following Dragičević et al. (Dragičević et al., 2019) Equation:

$$D_d = \frac{\sum_1^n L}{F} \quad (4)$$

Where, F is contributing drainage area (km^2), L is length of the waterway (km), n is number of waterways. Bathymetry and LULC data was collected from U.S. Geological Survey. The data from the DEM is used to calculate the TWI, as outlined by Kopecký et al. (2021) with measurements aligned to the grid unit of the DEM. TWI is computed using the Equation 5 suggested by Beven and Kirkby (1979), i.e :

$$TWI = \ln\left(\frac{\alpha}{\tan\beta}\right) \quad (5)$$

where α represents the slope angle/gradient, α the upslope contributing area per unit contour length, and the combined tan(β) represents the slope/steepest downslope direction distribution frequency. As per Riley et al. (1999), the calculation of the TRI is achieved through Equation 6. This entails deducting the elevation of a central cell (value) from the elevations of adjacent cells.This entails deducting the elevation of a central cell (value) from the elevations of adjacent cells. The resulting differences were squared, summed, and then squared once more (Różycka et al., 2017). Initially, the elevation differences are summed up before being either multiplied or squared. Squaring the multiplied or squared amount once more yields the final TRI result (Habib, 2021).

$$TRI = \frac{1}{\cos(\tan\beta \times \frac{\pi}{180})} \quad (6)$$

The "focal statistics" tool computes a statistic for each input cell location based on values in a given neighborhood surrounding it. The cells' mean, minimum, and maximum values from adjacent cells are needed to compute the Topographic Roughness Index (TRI). By entering the required parameter in the "focal statistics" window, these numbers can be computed directly. Then, each cell's TRI values are determined by running the following program (Chowdhury, 2023; Dragičević et al., 2019): ('Mean_DEM.tif' - 'Min_DEM.tif') / ('Max_DEM.tif' - 'Min_DEM.tif'). SAVI was extracted from

Landsat 9 using Equation (7). The soil erodibility factor (k) is computed from the FAO Digital Soil Map of the World (DSMW) using the Equation (8) following Wischmeier et al. (1971) .

$$\text{SAVI} = ((\text{Band 5} - \text{Band 4}) / (\text{Band 5} + \text{Band 4} + 0.5)) \times (1.5) \quad (7)$$

$$k = \frac{2.1\times10^{-4}(12-\text{OM})M^{1.14}+3.25(s-2)+2.5(p-3)}{759.4} \quad (8)$$

Where M = (percent silt + percent sand) × (100 − percent clay), K = soil erodibility (tons-yr/MJ-mm), OM = percentage organic matter, p = soil permeability code, and s = soil structure code.

3.1.3 Exposure Indicators

In this study the population density, elderly population (age > 65 years), younger population (age < 10 years), road network density was selected as exposure indicators based on expert opinions. The population density, elderly population, younger population data were collected from BBS report 2022. Additionally, the Local Government Engineering Department (LGED) provided the road network data, which was then extracted in a GIS system using ArcGIS Pro 3.2.

3.2 SMCDA Approach

3.2.1 Normalizing the values of indicators

As the quantity and dimensions of each incoming data set differ, normalization to a range of zero to one is necessary for their integration into SMCDA (Yoon, 2012) (Figure 3). This study employed two Equations (9 and 10) based on a min-max rescaling approach to normalize the hazard, vulnerability and exposure component values (Cutter et al., 2010; Kablan et al., 2017).

$$\boldsymbol{X_i} = \frac{\boldsymbol{x_i} - \boldsymbol{x_{max}}}{\boldsymbol{x_{max}} - \boldsymbol{x_{min}}} \quad (9) \qquad \boldsymbol{X_i} = \frac{\boldsymbol{x_{max}} - \boldsymbol{x_i}}{\boldsymbol{x_{max}} - \boldsymbol{x_{min}}} \quad (10)$$

$\boldsymbol{X_i}$ represents the normalized value of indicator i; $\boldsymbol{x_i}$ denotes the actual value of indicator i; $\boldsymbol{x_{max}}$ and $\boldsymbol{x_{min}}$ correspond to the maximum and minimum values, respectively, of indicators.

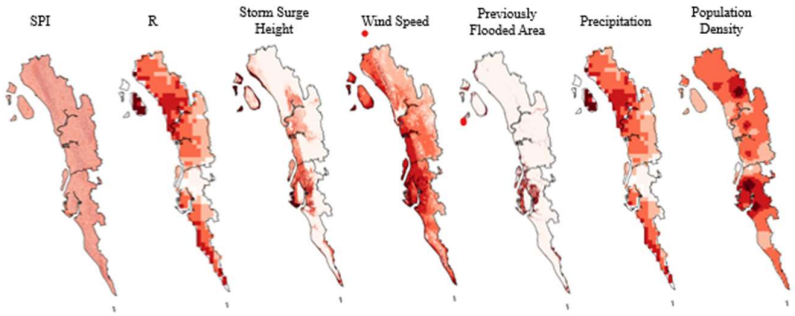

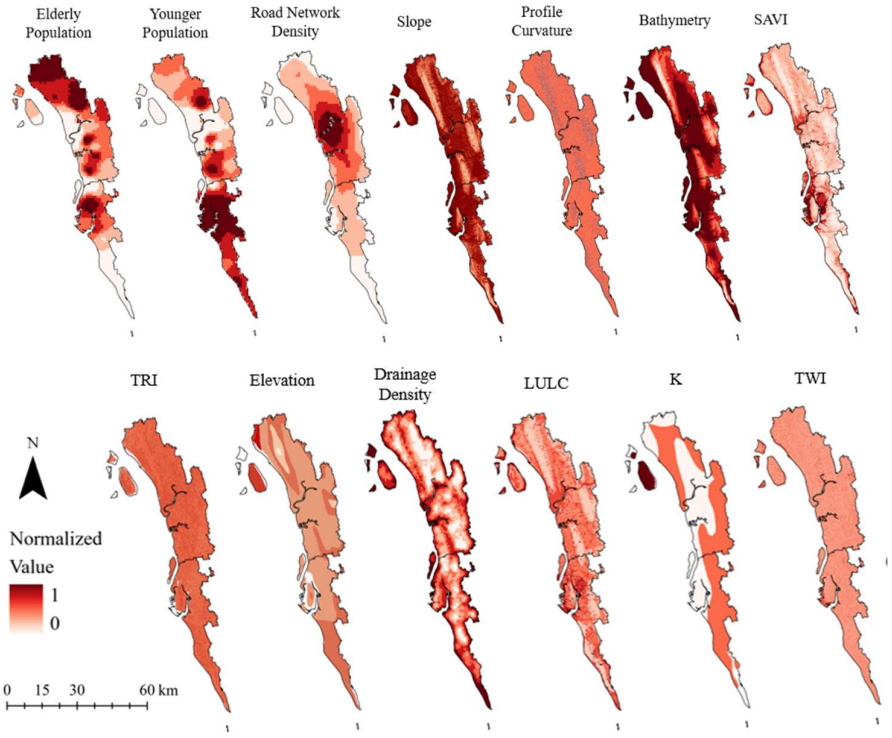

Figure 03: Spatial distributions of all the indicators

3.2.2 AHP Modelling for Weighting Indicators

The first stage in the AHP approach is to organize the MCDA problem into a hierarchical shape. A pairwise comparison is then carried out at every level in order to create a decision matrix. This procedure ensures efficient and clear processing by turning qualitative data into a definite value.(Deng, 1999; Hadipour el at., 2020). A standardized measurement scale from 1 to 9 was created by Saaty (1980) for the purpose of establishing a pairwise comparison matrix (PCM). A rating of 1 signifies equal importance, 9 designates significantly greater importance, and 1/9 indicates markedly lesser importance (Table 1).

Table 01: Linear scale for pairwise comparison of importance among the indicators (Saaty, 1980)

Decreasing the value for less importance				Equally important	Increasing the value for more importance			
1/9	1/7	1/5	1/3	1	3	5	7	9

Equation (11) shows the PCM of n criteria as follows (Saaty, 1980):

$$A = \begin{bmatrix} a_{11} & a_{12} & \dots & a_{1n} \\ a_{21} & a_{22} & \dots & a_{2n} \\ \dots & \dots & \dots & \dots \\ a_{m1} & a_{m2} & \dots & a_{mn} \end{bmatrix}, a_{ii} = 1,\ a_{ji} = \frac{1}{a_{ij}}, a_{ij} \neq 0 \qquad (11)$$

The reciprocal matrix is addressed using an eigenvector technique to ascertain the relative importance of criterion (Hadipour el at., 2020). The AHP quality outputs can be assessed through the consistency of the PCM. Equation (12) is therefore used to determine the consistency index (CI) (Saaty, 1980):

$$CI = \frac{\lambda_{max} - n}{n - 1} \qquad (12) \qquad CR = \frac{CI}{RI} \qquad (13)$$

Where λ max and n represent the maximum eigenvalue and the order of matrix A, respectively. Subsequently, the final consistency ratio (CR) is computed based on Saaty (Saaty, 1980). Here, RI stands for a random index, specifically, the consistency index of a randomly PCM. This index is contingent on the number of criteria (N) under comparison (Table 2).

Table 02: RI value for compute the CI (Saaty, 1980)

N	1	2	3	4	5	6	7	8	9	10	11
RI	0	0	0.58	0.9	1.12	1.24	1.32	1.41	1.45	1.49	1.51

It is advisable for CR values to be below 0.1; in cases where CR exceeds this threshold, it indicates inconsistency in pairwise comparisons, necessitating a revision of judgments to ensure meaningful results. In this study, the calculation of indicator weights involved distributing questionnaires to seven individuals (academia: three individuals; government agencies: two individuals; and national and local research institutions: two individuals) with specialization in coastal engineering, disaster management, spatial analysis, and climate change to ensure a diverse range of opinions. Subsequently, the experts were interviewed to provide their judgments by completing the questionnaire. The integration of individual judgments was achieved through the application of the geometric mean.

3.2.3 Aggregation Approach

Weighted Linear Combination (WLC) is a frequently used aggregation method in SMCDA, which functions as a simple overlay technique (Hadipour et al., 2020; Vafai et al., 2013). This method is easily comprehensible for decisionmakers and is compatible with spatial data (Malczewski, 2006). Individual application of the WLC model was carried out for every risk factor (hazard, vulnerability, and exposure) to create indexes, as outlined by Equation (14) following Malczewski (Malczewski, 2006).

$$Rc = \sum_{i=1}^{n} X_i \times W_i \quad (14)$$

Here, Rc shows how much each risk component is worth, W_i indicates the weight given to each indicator that was obtained using the AHP (where $W_i<1$ and $\sum_{i=1}^{n} W_i=1$), and X_i represents the normalized variables. In the end, as was previously indicated, the computed value for each component risk is an input for the risk formulation (Equation (1)) in order to create a coastal flooding risk index. Results and Discussions

4. RESULTS AND DISCUSSIONS

4.1 Analysis of Hazard

Six distinct indications were taken into consideration in order to examine the first risk component, flood hazard: storm surge inundation, SPI, rainfall erosivity factor (R) and wind speed set-up. Utilizing geospatial techniques, this study generated flood hazard maps, incorporating weights for indicators calculated through the AHP model (Table 3). Additionally, the CR of the flood hazard PCM fell within an acceptable range which is 0.05.

Table 03: PCM of hazard indicators

Hazard	H1	H2	H3	H4	H5	H6	Criteria Weight
H1	1	3	4	1	2	1	0.24
H2	1/3	1	3	1/3	1	1/3	0.10
H3	1/4	1/3	1	1/7	1/3	1/4	0.05
H4	1	3	7	1	1	1/3	0.20
H5	1/2	1	3	1	1	1	0.15
H6	1	3	4	3	1	1	0.26

H1=Precipitation, H2=Stream Power Index (SPI), H3=Rainfall Erosivity Factor (R), H4=Storm Surge Height, H5=Wind Speed and Direction, H6=Previously Flooded Area

Figure 4 displays the flood hazard zone, which is divided into five classifications from very low to very high. The very low, low, moderate, high, and very high zones encompass approximately 23.06%, 31.9%, 27.48%, 12.89%, and 4.66% respectively.

4.2 Analysis of Vulnerability

Ten indicators were chosen for vulnerability analysis and they are slope, elevation, profile curvature, drainage density, bathymetry, LULC, TRI, TWI, soil erodibility factor (K) and SAVI. The vulnerability component was equally applied to how the flood hazard component was processed to assess the relative significance of indicators that are vulnerable, as indicated in Table 4.

Table 04: PCM of vulnerability indicators

Vulnerability	V1	V2	V3	V4	V5	V6	V7	V8	V9	V10	Criteria Weight
V1	1	3	1/3	3	3	1/3	1/5	3	1/3	1	0.08
V2	1/3	1	1	3	3	1/5	1/5	2	1/3	3	0.07
V3	3	1	1	1	4	1/3	1/5	3	3	3	0.11
V4	1/3	1/3	1	1	3	1/7	1/7	1	1/3	2	0.05
V5	1/3	1/3	1/4	1/3	1	1/5	1/5	1	1/3	1	0.03
V6	3	5	3	7	5	1	3	6	3	5	0.26
V7	5	5	5	7	5	1/3	1	5	3	3	0.22
V8	1/3	1/2	1/3	1	1	1/6	1/5	1	1/3	1/2	0.03
V9	3	3	1/3	3	3	1/3	1/3	3	1	3	0.11
V10	1	1/3	1/3	1/2	1	1/5	1/3	2	1/3	1	0.04

V1=Slope, V2=Profile Curvature, V3=Bathymetry, V4=SAVI, V5=TRI, V6=Elevation, V7=Drainage Density, V8=LULC, V9=Soil Erosivity Factor (K), V10=Topographic Wetness Index (TWI)

The calculated CR value for the vulnerability matrix was 0.08, suggesting that the weights assigned to indicators are appropriate to create the vulnerability index and the classifications of vulnerability zones are shown in Figure 4. Among the five classes very low, low, moderate, high and very high zones cover about 25.67%, 16.16%, 27.97%, 19.79% and 10.41% respectively.

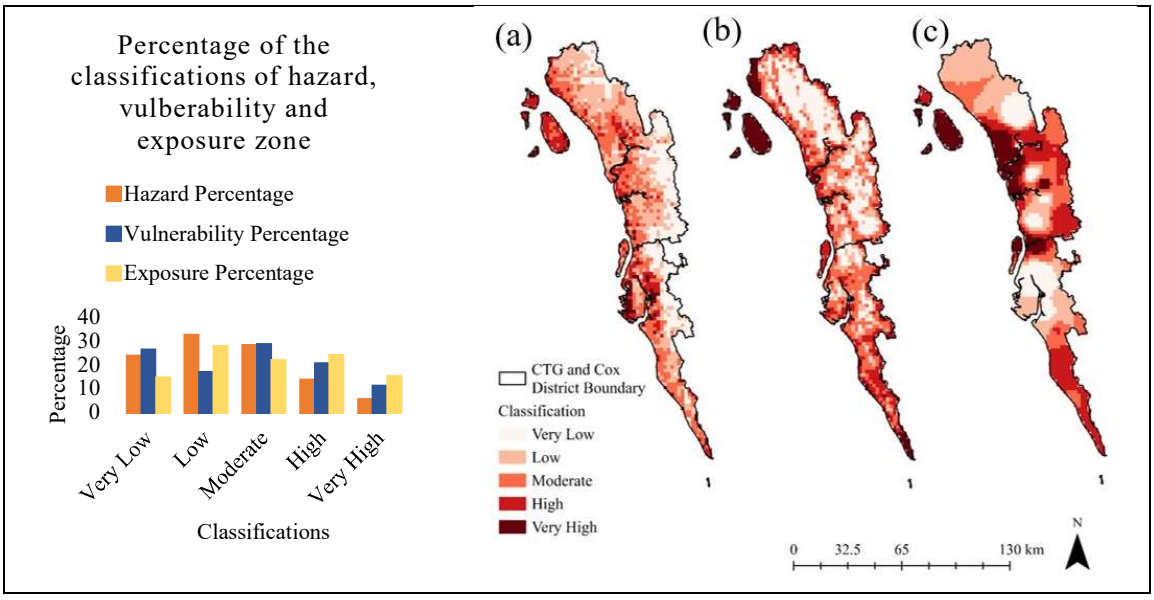

Figure 04: Spatial distribution and classifications of flood hazard (a), vulnerability (b) and exposure (c) zones

4.3 Analysis of Exposure

The flood exposure map in this study was created using a normalized value of population density, elderly population (age > 65 years), younger population (age < 10 years), road network density. The

PCM is shown in Table 5 along with the criteria weight. The CR value is 0.04 which is accepted. The spatial distribution of exposure zone is shown in Figure 4 with five distributed classes: very low (13.86%), low (27.18), moderate (21.07%), high (23.49%) and very high (14.14%).

Table 05: PCM of exposure indicators

Exposure	E1	E2	E3	E4	Criteria Weight
E1	1	1/3	1/3	3	0.16
E2	3	1	1	5	0.40
E3	3	1	1	3	0.36
E4	1/3	1/5	1/3	1	0.08

E1=Population Density, E2=Elderly Population, E3=Younger Population, E4=Road Network Density

4.4 Final Result and Validation

The final goal of this study was toTo evaluate the risk posed to individuals in flood scenarios, GIS was employed to integrate flood hazards, vulnerability, and exposure maps. Figure 5 shows the five classes into which the flood risk zone was divided, along with the percentages of the very low (42.74%), low (12.77%), moderate (10.35%), high (25.91%), and very high (8.23%) zones. The high and very high zone have covered the Chattogram City Corporation area, Sandwip, Anwara, Bashkhali, Satkania, Moheshkhali upazilas in Chattogram district. And in Cox's Bazar district the Cox's Bazar Sadar, Ukhia upazila are under high and very high risk zones.

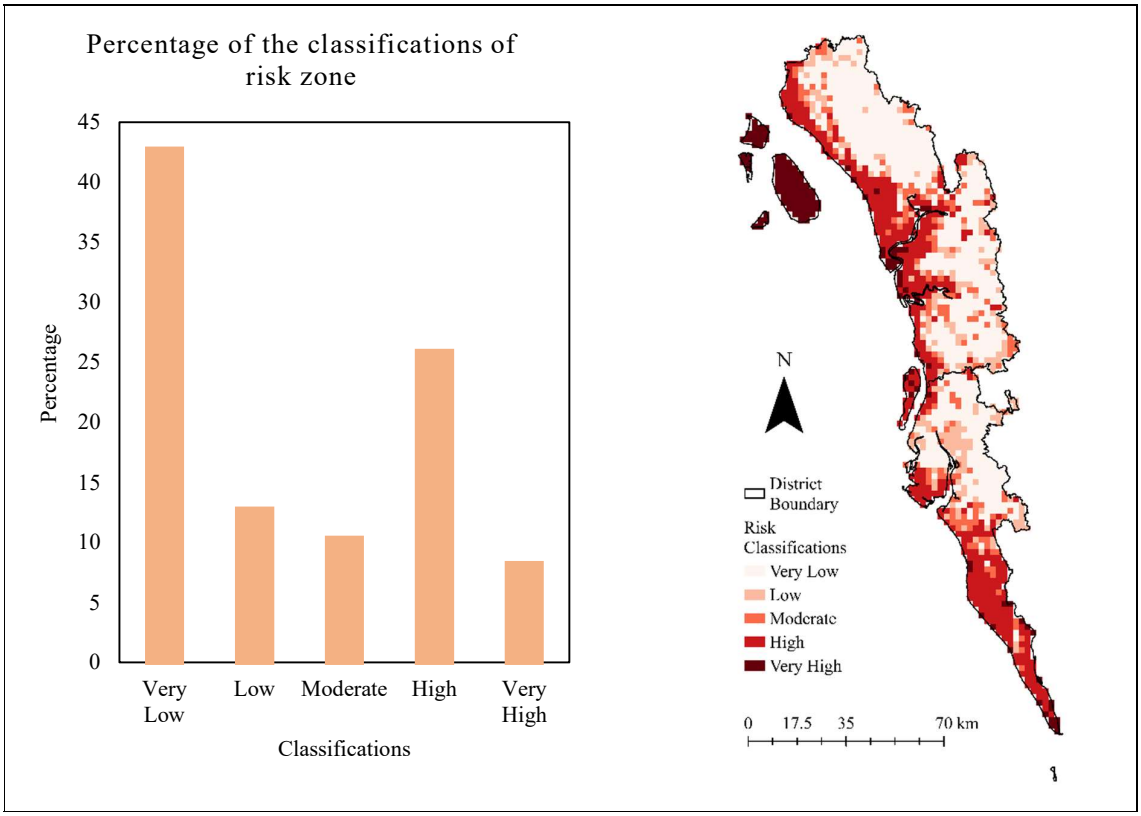

Figure 05: Spatial distribution and classifications of flood risk zones

In order to validate the map, historical flood inventory data was compared with the flood risk map using the Area Under the Curve (AUC). The cumulative percentage of flood occurrences was computed, yielding an average AUC ratio of 83.51% (Figure 6). This indicates that the final outcome of the flood risk analysis conducted demonstrate a high level of reliability, falling within the range of 0.8 to 0.9 for

the AUC (Wang et al., 2010). The final output shows that 25.91% of total area in this study is under high risk zone and 8.23% is under very high risk zone.

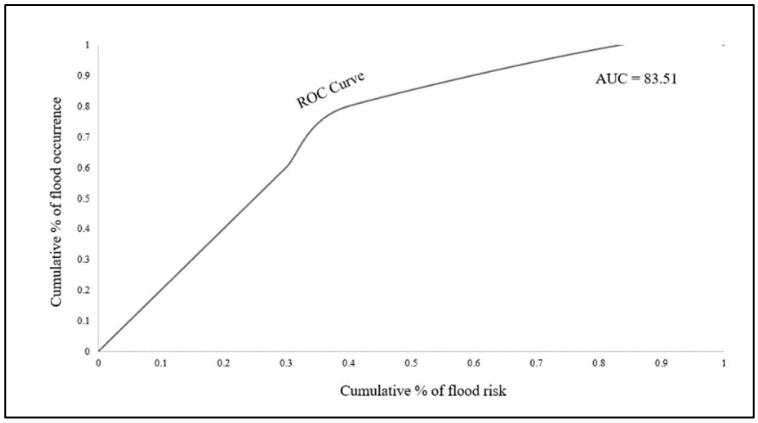

Figure 06: Validation of flood risk map with Area Under the Curve (AUC)

5. CONCLUSION

The semiquantitative approach employes in this study reasoably develops the flood risk index weights. This approach is particularly helpful in limited data availability and dependability issues make it difficult to simulate coastal floods and create physical vulnerability curves using statistical approaches and physical model running. Essentially, expensive, time-consuming, and sophisticated quantitative models could be avoided by the integration of weighted indicators and related proxy variables, depending on expert views. Since many of the qualitative and quantitative indicators have used to map flood risk are dynamic, SMCDA exhibits flexibility in managing a large number of them. It may also be updated on a regular basis by adding or changing indicators as needed. Sensitivity analysis requires to evaluate the model's correctness in the data scarce flood prone coasts. The SMCDA produced flood risk map and offers a thorough database. Thus, stakeholders and decision-makers create plans for mitigating the danger of flooding. Therefore, the final map can serve as a useful tool for decision-makers to improve land zoning for the efficient flood risk management techniques.

ACKNOWLEDGEMENTS

The authors are grateful to the Chittagong University of Engineering and Technology (CUET), Bangladesh, for providing funds to conduct a project titled Characterizing Compound flooding effect in Bangladesh Coast (COMPOUND FLOODING) CUET/DRE/2021-22/WRE/003. Logistic helps from the BWDB, BMD are also appreciated.

REFERENCES

Abbass, K., Qasim, M. Z., Song, H., Murshed, M., Mahmood, H., & Younis, I. (2022). A review of the global climate change impacts, adaptation, and sustainable mitigation measures. Environmental Science and Pollution Research, 29(28), 42539–42559. https://doi.org/10.1007/s11356-022-19718-6

Adnan, M. S. G., Haque, A., & Hall, J. W. (2019). Have coastal embankments reduced flooding in Bangladesh? Science of The Total Environment, 682, 405–416. https://doi.org/10.1016/j.scitotenv.2019.05.048

AlAli, A. M., Salih, A., & Hassaballa, A. (2023). Geospatial-Based Analytical Hierarchy Process (AHP) and Weighted Product Model (WPM) Techniques for Mapping and Assessing Flood

Susceptibility in the Wadi Hanifah Drainage Basin, Riyadh Region, Saudi Arabia. Water, 15(10), 1943. https://doi.org/10.3390/w15101943

Basher, R. (2009). UNISDR Terminology on Disaster Risk Reduction (2009).

BBS. (2023). Population and Housing Census 2022. Bangladesh Bureau of Statistics (BBS), Statistics & Informatics Division(SID), Ministry of Planning, Government of the People's Republic of Bangladesh. https://bbs.portal.gov.bd

Beven, K. J., & Kirkby, M. J. (1979). A physically based, variable contributing area model of basin hydrology / Un modèle à base physique de zone d'appel variable de l'hydrologie du bassin versant. Hydrological Sciences Bulletin, 24(1), 43–69. https://doi.org/10.1080/02626667909491834

Bhuiyan, A. H., Darda, A., Habib, W., & Hossain, B. (2020). Marine Tourism for Sustainable Development in Cox's Bazar, Bangladesh. Asian Development Bank Institute.

Cai, S., Fan, J., & Yang, W. (2021). Flooding Risk Assessment and Analysis Based on GIS and the TFN-AHP Method: A Case Study of Chongqing, China. Atmosphere, 12(5), 623. https://doi.org/10.3390/atmos12050623

Chowdhury, Md. S. (2023). Modelling hydrological factors from DEM using GIS. MethodsX, 10, 102062. https://doi.org/10.1016/j.mex.2023.102062

Coastal Zone Policy 2005. | UNEP Law and Environment Assistance Platform. (n.d.). Retrieved December 14, 2023, from https://leap.unep.org/en/countries/bd/national-legislation/coastal-zone-policy-2005

Dano, U., Balogun, A.-L., Matori, A.-N., Wan Yusouf, K., Abubakar, I., Said Mohamed, M., Aina, Y., & Pradhan, B. (2019). Flood Susceptibility Mapping Using GIS-Based Analytic Network Process: A Case Study of Perlis, Malaysia. Water, 11(3), 615. https://doi.org/10.3390/w11030615

Danumah, J. H., Odai, S. N., Saley, B. M., Szarzynski, J., Thiel, M., Kwaku, A., Kouame, F. K., & Akpa, L. Y. (2016). Flood risk assessment and mapping in Abidjan district using multi-criteria analysis (AHP) model and geoinformation techniques, (cote d'ivoire). Geoenvironmental Disasters, 3(1), 10. https://doi.org/10.1186/s40677-016-0044-y

Deng, H. (1999). Multicriteria analysis with fuzzy pairwise comparison. International Journal of Approximate Reasoning, 21(3), 215–231. https://doi.org/10.1016/S0888-613X(99)00025-0

Dragičević, N., Karleuša, B., & Ožanić, N. (2019). Different Approaches to Estimation of Drainage Density and Their Effect on the Erosion Potential Method. Water, 11(3), 593. https://doi.org/10.3390/w11030593

Faiz Ahmed, C., School of Planning and Architecture, Vijayawada 521104, Andhra Pradesh; India, & Kranthi, N. (2018). Flood Vulnerability Assessment using Geospatial Techniques: Chennai, India. Indian Journal of Science and Technology, 11(6), 1–13. https://doi.org/10.17485/ijst/2018/v11i6/110831

Field, C. B., Barros, V., Stocker, T. F., & Dahe, Q. (Eds.). (2012). Managing the Risks of Extreme Events and Disasters to Advance Climate Change Adaptation: Special Report of the Intergovernmental Panel on Climate Change (1st ed.). Cambridge University Press. https://doi.org/10.1017/CBO9781139177245

Habib, M. (2021). Quantifying Topographic Ruggedness Using Principal Component Analysis. Advances in Civil Engineering, 2021, 1–20. https://doi.org/10.1155/2021/3311912

Hadipour, A., Vafaie, F., & Hadipour, V. (2015). Land suitability evaluation for brackish water aquaculture development in coastal area of Hormozgan, Iran. Aquaculture International, 23(1), 329–343. https://doi.org/10.1007/s10499-014-9818-y

Hadipour, V., Vafaie, F., & Deilami, K. (2020). Coastal Flooding Risk Assessment Using a GIS-Based Spatial Multi-Criteria Decision Analysis Approach. Water, 12(9), 2379. https://doi.org/10.3390/w12092379

Hadipour, V., Vafaie, F., & Kerle, N. (2020). An indicator-based approach to assess social vulnerability of coastal areas to sea-level rise and flooding: A case study of Bandar Abbas city, Iran. Ocean & Coastal Management, 188, 105077. https://doi.org/10.1016/j.ocecoaman.2019.105077

Hossain, M. Z., & Adhikary, S. K. (2022). Flood Susceptibility Assessment In Southwest Coastal Region Of Bangladesh Using An Ahp-Gis Based Approach.

Jaafari, A., Najafi, A., Pourghasemi, H. R., Rezaeian, J., & Sattarian, A. (2014). GIS-based frequency ratio and index of entropy models for landslide susceptibility assessment in the Caspian forest, northern Iran. International Journal of Environmental Science and Technology, 11(4), 909–926. https://doi.org/10.1007/s13762-013-0464-0

Kopecký, M., Macek, M., & Wild, J. (2021). Topographic Wetness Index calculation guidelines based on measured soil moisture and plant species composition. Science of The Total Environment, 757, 143785. https://doi.org/10.1016/j.scitotenv.2020.143785

Li, Y., Martinis, S., Wieland, M., Schlaffer, S., & Natsuaki, R. (2019). Urban Flood Mapping Using SAR Intensity and Interferometric Coherence via Bayesian Network Fusion. Remote Sensing, 11(19), 2231. https://doi.org/10.3390/rs11192231

Liu, K., Li, Z., Yao, C., Chen, J., Zhang, K., & Saifullah, M. (2016). Coupling the k-nearest neighbor procedure with the Kalman filter for real-time updating of the hydraulic model in flood forecasting. International Journal of Sediment Research, 31(2), 149–158. https://doi.org/10.1016/j.ijsrc.2016.02.002

Malczewski, J. (2006). GIS-based multicriteria decision analysis: A survey of the literature. International Journal of Geographical Information Science, 20(7), 703–726. https://doi.org/10.1080/13658810600661508

MORGAN, R. (1974). Estimating Regional Variations In Soil Erosion Hazard In Peninsular Malaysia. Malayan Nature Journal, 28(2), 94–106.

Murshed, S., Griffin, A. L., Islam, M. A., Wang, X. H., & Paull, D. (2022). Assessing multi-climate-hazard threat in the coastal region of Bangladesh by combining influential environmental and anthropogenic factors. Progress in Disaster Science, 16, 100261. https://doi.org/10.1016/j.pdisas.2022.100261

Pradhan, B. (2009). Flood susceptible mapping and risk area delineation using logistic regression, GIS and remote sensing. Journal of Spatial Hydrology, 9, 1–18.

Rahmati, O., Kalantari, Z., Samadi, M., Uuemaai, E., Moghaddam, D. D., Nalivan, O. A., Destouni, G., & Tien Bui, D. (2019). GIS-Based Site Selection for Check Dams in Watersheds: Considering Geomorphometric and Topo-Hydrological Factors. Sustainability, 11(20), 5639. https://doi.org/10.3390/su11205639

Riley, S., Degloria, S., & Elliot, S. D. (1999). A Terrain Ruggedness Index that Quantifies Topographic Heterogeneity. Internation Journal of Science, 5, 23–27.

Różycka, M., Migoń, P., & Michniewicz, A. (2017). Topographic Wetness Index and Terrain Ruggedness Index in geomorphic characterisation of landslide terrains, on examples from the Sudetes, SW Poland. Zeitschrift Für Geomorphologie, Supplementary Issues, 61(2), 61–80. https://doi.org/10.1127/zfg_suppl/2016/0328

Saaty, T. L. (1980). The analytic hierarchy process: Planning, priority setting, resource allocation. McGraw-Hill International Book Co. http://www.gbv.de

Shafapour Tehrany, M., Shabani, F., Neamah Jebur, M., Hong, H., Chen, W., & Xie, X. (2017). GIS-based spatial prediction of flood prone areas using standalone frequency ratio, logistic regression, weight of evidence and their ensemble techniques. Geomatics, Natural Hazards and Risk, 8(2), 1538–1561. https://doi.org/10.1080/19475705.2017.1362038

Siahkamari, S., Haghizadeh, A., Zeinivand, H., Tahmasebipour, N., & Rahmati, O. (2018). Spatial prediction of flood-susceptible areas using frequency ratio and maximum entropy models. Geocarto International, 33(9), 927–941. https://doi.org/10.1080/10106049.2017.1316780

Souissi, D., Zouhri, L., Hammami, S., Msaddek, M. H., Zghibi, A., & Dlala, M. (2020). GIS-based MCDM – AHP modeling for flood susceptibility mapping of arid areas, southeastern Tunisia. Geocarto International, 35(9), 991–1017. https://doi.org/10.1080/10106049.2019.1566405

Teng, J., Jakeman, A. J., Vaze, J., Croke, B. F. W., Dutta, D., & Kim, S. (2017). Flood inundation modelling: A review of methods, recent advances and uncertainty analysis. Environmental Modelling & Software, 90, 201–216. https://doi.org/10.1016/j.envsoft.2017.01.006

UNICEF, U. (2023, September). Bangladesh Humanitarian Situation Report No.2 (Floods and Landslides in Chittagong and Cox's Bazar) 5 September 2023 | UNICEF. https://www.unicef.org

Vafai, F., Hadipour, V., & Hadipour, A. (2013). Determination of shoreline sensitivity to oil spills by use of GIS and fuzzy model. Case study – The coastal areas of Caspian Sea in north of Iran. Ocean & Coastal Management, 71, 123–130. https://doi.org/10.1016/j.ocecoaman.2012.05.033

Wang, N., Zeng, N. N., & Zhu, W. (2010). Sensitivity, Specificity, Accuracy, Associated Confidence Interval And ROC Analysis With Practical SAS Implementations.

Wheater, H. S. (2006). Flood hazard and management: A UK perspective. Philosophical Transactions of the Royal Society A: Mathematical, Physical and Engineering Sciences, 364(1845), 2135–2145. https://doi.org/10.1098/rsta.2006.1817

Wischmeier, W. H., Johnson, C. B., & Cross, B. V. (1971). Soil Erodibility Nomograph For Farmland And Construction Sites. https://trid.trb.org/view/125184

Yoon, D. K. (2012). Assessment of social vulnerability to natural disasters: A comparative study. Natural Hazards, 63(2), 823–843. https://doi.org/10.1007/s11069-012-0189-2